CIMAC CONGRESS 25
ZURICH, MAY 19 – 23, 2025

2025 | 102

Investigation of port fuel injected methanol and its aftertreatment concepts

Emission Reduction Technologies - Engine Measures & Combustion Development

Martin Axelsson, Wärtsilä

Omer Faruk Atac, Wärtsilä
Viktor Heir, Wärtsilä

ABSTRACT

The shipping industry is actively exploring alternative fuels to reduce its environmental impacts. Methanol has emerged as a promising option to decrease greenhouse gas emissions. By utilizing green methanol as a fuel in a combustion engine, the industry can make significant progress towards achieving its carbon reduction goals.

Methanol has a lower heating value compared with traditional fossil fuels, necessitating larger storage capacities. As a result, more methanol is required to achieve the same energy content as fossil fuels. The larger injected quantity, higher latent heat of vaporization, lower viscosity and density compered traditional fossil liquid fuels necessitate thorough optimization of the methanol injection system, especially injector location, spray orientation and spray characteristic etc.

Though methanol is considered a climate friendlier alternative to fossil fuels, it still produces emissions such as carbon dioxide, nitrogen oxides, particulate matter, formaldehyde and in case of urea in an SCR system also hydrogen cyanide. Based on preliminary investigations, the partly burned emissions are found to be unexpectedly high, thus necessitating an appropriate aftertreatment solutions.

To address the issues mentioned above, this paper aims to provide a comprehensive review of the concept of methanol combustion with port fuel injection based on engine test results, focusing on methanol spray optimization, emissions and efficiency. In this study, several PFI injectors were tested to achieve better atomization performance, thus improved mixing and combustion process. The experimental investigations are done both on a medium-speed four-stroke engine and in a spray rig. Based on the results, it was found that atomization performance has only a small effect on the emissions even if spray characteristic is improved significantly. In addition, the partly burned emissions are found to be higher than expected with pre-mixed PFI methanol combustion with all tested setups. In that sense, potential aftertreatment solutions for methanol combustion with port fuel injection are explored and appropriate aftertreatment technologies are discussed and suggested to minimize the environmental impact of methanol combustion further.

Based on the findings, this study can provide important insight on utilization of the methanol engine efficiently by investigating port fuel injected methanol and its potential aftertreatment solutions considering regulated and unregulated emissions. Moreover, some of key issues associated with using methanol as fuel in combustion engines, such as cylinder wall wetting and lube oil contamination, are also discussed additionally in this article.

1 INTRODUCTION

To achieve the global goal of reaching net-zero greenhouse gas (GHG) emissions in international shipping by 2030 and 2050 [1], engine manufacturers have extensively researched the use of alternative fuels such as methanol, ammonia, and hydrogen for marine engines [2-4]. Among such alternative fuels, methanol has been identified as a promising option for reducing greenhouse gas emissions in the short term [5]. This is due to its known characteristics as a fuel for internal combustion engine (ICE), including higher latent heat of vaporization, lower cetane number, lower stoichiometric air-fuel ratio, and reduced combustion temperature. Additionally, it remains in liquid form at ambient pressure and temperature, which facilitates its storage and transportation. From this end, methanol, as an alternative fuel, offers several advantages for marine applications when compared to other options, particularly in terms of storage, handling, and combustion process [6]. In addition to these advantages, the availability of alternative fuels is an important aspect to highlight. Methanol serves as both an energy carrier and a base chemical for industrial applications. It is produced using both traditional methods (from natural gas) and synthetic methods (from renewable sources and bio-based materials), resulting in a high production rate and widespread availability globally compared to various other fuels.

Several methods have been employed to utilise methanol in internal combustion engines, including direct methanol injection (direct injection (DI) approach) [7,8], blending methanol with diesel fuel [9,10], and injecting methanol into the intake port (port fuel injection (PFI) approach) [11,12]. It is well-established that the DI approach offers good engine efficiency compared to the PFI approach [13]. Additionally, the diffusion combustion characteristics inherent to the DI approach would effectively minimize the interactions between fuel spray and the cylinder liner walls. This reduction significantly mitigates problems associated with engine oil contamination compared to PFI. On the other hand, such approach requires relatively higher injection pressure and much more complex fuel injection system. As a result, the cost of the fuel systems significantly increases.

Conversely, PFI injection offers a potentially cost-effective solution for methanol fuel supply due to its low fuel pressure requirements. This reduced fuel pressure allows the entire system—including the injector, fuel pump, and piping—to be compact and comparatively simple. Additionally, PFI is more viable as a retrofit option because of its simplicity and significantly lower cost in comparison to high-pressure DI systems.

In the PFI approach, it is important to note that the wall wetting and corresponding risks of lube oil contamination increase significantly. These problems are primarily attributed to the injector location, spray orientation, and spray characteristics. Among these factors, spray characteristics have a considerable impact on such issues. Poor atomization performance (resulting in larger droplets) of the fuel spray in the intake port is more likely to cause wall wetting rather than seamlessly integrating with the intake air. To minimize wall wetting in the intake port and prevent wall impingement on the cylinder liner, which leads to lube oil contamination, it is essential to enhance the atomization performance of the spray in conjunction with other factors.

From the pollutant emissions standpoint, methanol can be considered as climate friendly alternative to fossil fuels, but it can still produce regulated emissions such as carbon dioxide (CO_2), carbon monoxide (CO), nitrogen oxides (NO_x), hydrocarbon (HC), particulate matter (PM) [14,15]. Moreover, unregulated emissions, particularly formaldehyde (CH_2O) [16,17]. Formaldehyde is well-known for its high toxicity and carcinogenic properties; thus, it poses a significant threat to human health. Our preliminary investigations indicated that the levels of partially burned emissions appeared to be unexpectedly high. Therefore, the implementation of suitable aftertreatment solutions is imperative. When utilizing urea in a Selective Catalytic Reduction (SCR) [18] aftertreatment system, the formation of substances such as hydrogen cyanide (*HCN*) may occur. It is crucial to consider such highly toxic substances during the aftertreatment process.

The present study aims to develop a thorough understanding of the port fuel injected methanol concept and its associated aftertreatment methodologies to minimize both regulated and unregulated emissions. To achieve this, an optical diagnostic investigation was first conducted on the spray characteristics of three different PFI injectors using a spray rig. These observations were then correlated with engine performance and emissions on a medium-speed four-stroke test engine. During the engine tests, emission characteristics such as carbon dioxide, nitrogen oxides, and formaldehyde were examined. The potential mitigation of these emissions by aftertreatment solution is evaluated. An oxidation catalyst is examined and its impact on emission characteristics and conversion efficiency is evaluated on the test engine with respect to exhaust gas temperature. Potential issues related to SCR while having a relatively high methanol slip is also discussed. Finally, the combination of engine and oxidation catalyst performance with the best injector is evaluated. The overall performance

when methanol share is maximized, and a small oxidation catalyst is introduced is compared to the case when emissions are instead minimized from combustion itself without using any oxidation catalyst.

2 EXPERIMENTAL METHODOLOGIES

2.1 Experimental Setup for Spray Characterizations

In this study, diffused backlight illumination (DBI) method is utilized to investigate spray atomization characteristics of PFI injectors both qualitatively and quantitively. As shown in Figure 1, in this method, experimental set up consists of light source, diffuser, injector and camera. To obtain spray morphology images at downstream (macroscopic spray imaging), LED light source is used with diffuser for uniform light distribution and such morphological spray motion are frozen with high speed/low resolution camera (Figure 1(a)). For capturing spray droplets imaging, sub-second pulsed laser light source, which is required to freeze the droplets motion, was applied with high resolution/low speed PCI camera. Also, a long-distance microscope is used to magnify the optical field for detecting sufficient droplets at the region of interest. In the DBI method [19], when the strong uniform light hits the back of the spray object, a bright background is created. The refracted light disperses, making the liquid interface look dark. Thus, shadowgraph images were generated with bright spray background and dark liquid/gas interfaces (appears based on different refracted index).

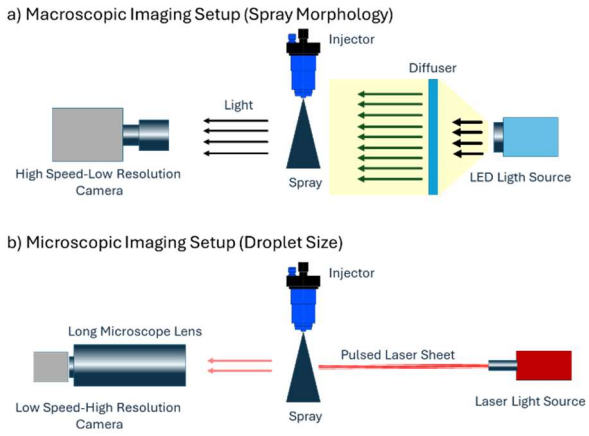

Figure 1. Experimental set up for spray visualization using diffuse back light illumination; a) Macroscopic spray imaging for spray morphology, b) Microscopic spray imaging for spray droplets.

In addition to the optical setup, the test liquid was pressurized using a gear pump capable of pressurizing liquid up to 200 bar. An accumulator with a damper element is placed on top of the injector to prevent pressure fluctuations during injection. A high-resolution pressure sensor is installed between the accumulator and the injector. The DeweSoft data acquisition platform was used to obtain the detected liquid pressure.

It is important to note that experimental studies of spray visualization of PFI injectors were conducted in an open environment, with ambient pressure and temperature, without a spray chamber. Water was used as the test liquid for this preliminary spray investigation. Applying methanol for this simple experimental investigation requires significant safety measures in the test room infrastructure. Therefore, water was used to gain initial insights into the spray breakup and atomization process of test injectors before testing them on the engine, although the breakup process may differ when using methanol.

As shown in Figure 2, three commercially available low-pressure PFI injectors were chosen for spray investigations. Injector A, an inwardly opening Injector A used for race cars, was tested with and without a hole plate at 4 bar injection pressure (Figure 2). Injector B is an inwardly opening low pressure atomizer, and Injector C is a pressure-swirl type injector. Both are used in marine and aerospace applications.

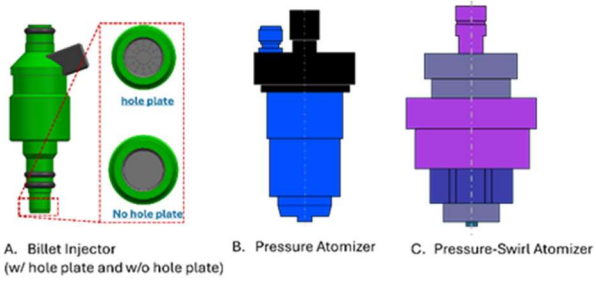

Figure 2. Selected low pressure PFI test injectors; a) billet injector (used particularly in race cars), b) pressure and c) pressure-swirl atomizers (used marine and aerospace applications).

The spray morphologies of injectors B and C were analyzed at far-field under varying injection pressure conditions. Each injector was tested within its operational range. Injector B was tested at pressures from 5 to 20 bar in 5-bar increments, while injector C was tested at pressures from 10 to 50 bar in 10-bar increments.

For injector C, the spray morphology in the near field was also examined to understand how swirling motion influences the primary breakup process of the spray. In addition to the analysis of spray morphology in both far- and near-field regions, microscopic visualization was performed for injector C to quantify droplet size at different axial locations under varying injection pressure conditions.

In the test, the injection durations are set to 13 ms for injector A, 10 ms for injector B, and 8 ms for injector C to meet the required fuel quantity for engine specifications. Table 1 provides a summary of the injection conditions.

Table 1. Injection conditions

Injection Conditions			
PFI Injector	Inj. A	Inj. B	Inj. C
Injection pressure [bar]	4	5-20	10-50
Ambient pressure [bar]	1	1	1
Ambient temperature [K]	298	298	298
Injection duration [ms]	13	10	8
Test liquid	H_2O	H_2O	H_2O

2.1.1 Quantifying Spray Cone Angle and Droplet Size via Image Processing

From the spray images obtained through both macroscopic and microscopic imaging techniques, we can quantify the spray cone angle and droplet size. The spray cone angle is defined as the angle between the spray boundaries. As illustrated in Figure 3(a), spray boundaries can be detected using a binarization method (Otsu method was employed in this study) on grayscale images. The binarization process allows the separation of the background from the spray image. After determining the spray boundaries, as shown in Figure 3(a), the spray dispersion angle—defined as the angle between the spray boundary and the injector axial direction—is calculated. Ultimately, the spray cone angle is determined by summing the spray dispersion angles (θ_R and θ_L) at the right side and left side of the boundary (Figure 3(a)). The spray cone angle measurement was done at 90-150 mm axial distance from the nozzle tip.

For droplet size measurement, similar to the spray angle measurement mentioned previously, the first step is to binarize grayscale droplet images using the Otsu method, as shown in Figure 3(b). Each droplet is then detected based on a circularity threshold set in the image processing algorithm. Subsequently, the area of each detected droplet is calculated and converted into actual size using image resolution information. These droplet areas are then converted into droplet diameters ($d_{droplet}$) using the equation for the area of a circle. Finally, the Sauter Mean Diameter (SMD, D_{Drop}) is calculated based on the equation shown in Figure 3(b).

It is pertinent to mention that consistent measurements for both spray angle and droplet size were achieved by averaging the results of 5 consecutive injections.

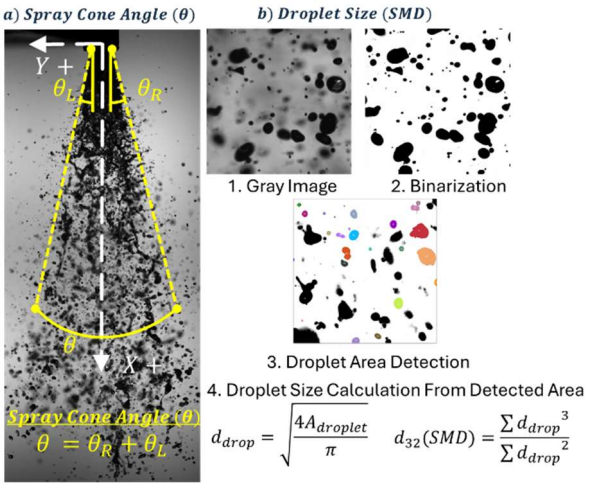

Figure 3. Calculation of spray cone angle and droplet size measurements.

2.2 Experimental Setup for Test Engine and Aftertreatment System

The research test engine is a medium speed 4-stroke in-line 6-cylinder engine based on Wärtsilä 20. The engine, excluding the power train, is modified to facilitate testing of new technologies and combustion systems. The engine has fully variable valve train, 2-stage serial turbo layout and common rail diesel fuel injection system. The main specification of the test engine is listed in table 2 and test layout is shown in figure 4.

Table 2. Test engine main specifications.

W6L20 Research Engine	**Specifications**
Bore	200 mm
Stroke	280 mm
Nomina speed and power	1000 rpm and 200 kW/cyl
Compression ratio	15:8
Turbo layout	2-stage in series
Diesel fuel system	Common rail
Methanol fuel system	Port fuel injection (up to 50 bar)
Valve train system	Fully variable

Emission system	Horiba Mexa (NO_x,CO,THC, CO_2, O_2) Gasmet FTIR GT6000 gas analy. (NO, NO_2, CH_3OH, CH_2O, CO, CO_2, H_2O) AVL415SE(FSN-Soot)

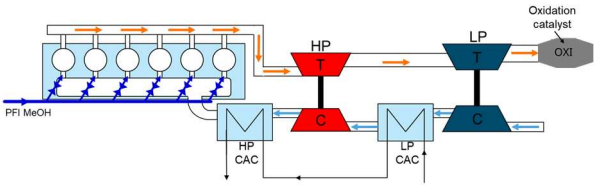

Figure 4. Schematic view of experimental setup for engine and aftertreatment.

The requirement of this test setup is to maintain pure diesel engine mode with minimum changes only necessary for enabling a fractional use of methanol. The reason for this, is to ensure optimum performance on diesel mode (with high compression ratio) since the availability of green methanol in short-to-midterm is limited. Additionally, a cost-effective retrofit for existing diesel engines is an attractive solution. However, the main drawback with this is that the maximum methanol fuel share is strongly limited by knocking, mainly because of the high compression ratio. Moreover, the fractional use of premixed methanol but with all air available (for the DI diesel to be injected) will subsequently result in ultra-lean premixed methanol mixture giving relatively high unburned and partly burned emissions while high NOx emissions inherent to the diffusion combustion will be produced from the later direct injected main diesel fuel. As such fuel-sharing combustion approach combines the emissions that are high for each combustion type, thus the need of aftertreatment is essential to provide overall low emissions of the concept.

In general, the oxidation catalyst is placed before the SCR however, in this particular study, no SCR was used (not needed for IMO Tier II only for IMO Tier III). Oxidation catalyst specification is reported in table 3.

Table 3. Oxidation catalyst specifications.

Oxidation Catalyst	Specifications
Substrate	Corrugated metal foil
Cell density	100 cpsi
Washcoat	PGM
Cell volume	28l

Each cylinder has one PFI injector in the intake port, i.e. multi point injection. The injector location is based on the findings from a CFD study where the focus is to minimize liner wetting, maximize trapped fuel in cylinder and homogeneity of fuel-air mixture. The engine has reverse flow cylinder head layout which makes proper positioning of a single injector challenging with many trade-offs. According to the CFD result, it is better to aim towards first valve instead of both, because it has much less swirl compared to the port/valve further away to avoid wall wetting inside cylinder but with worse mixing as drawback. To avoid excessive wall wetting and to empty intake port properly from fuel, the injector should be relatively close to intake valve. The drawback is the reduced time for mixing of fuel and air, and evaporation of methanol. The final PFI location for the engine test is illustrated in figure 5.

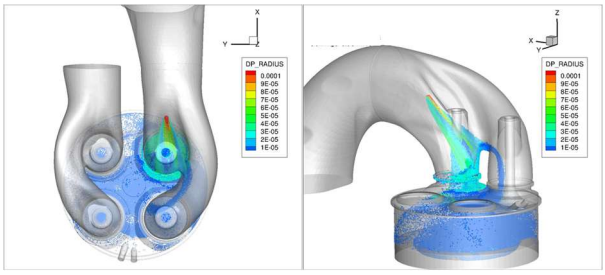

Figure 5. PFI location and illustration of the spray during intake stroke.

The location is the same for both injector A and C, but the length/penetration is different, where injector C is protruding into the intake port about 90 mm more than injector A. Whereas, Injector B was never tested on the engine since the spray pattern is similar to injector A and hence expected to have less impact on engine performance for providing clear test results.

3 RESULTS AND DISCUSSIONS

3.1 Spray Characterization of Different PFI Injectors and Droplet Size Measurement

3.1.1 Spray Morphology of Billet Injector at Far-field (Inj. A- w/hole plate and w/o hole plate)

As illustrated in Figure 6, the spray characteristics of the Injector A are evaluated with and without a hole plate at the nozzle exit under an injection pressure of 4 bar. Without the hole plate, the spray appears as a liquid core with minimal breakup processes, except for some surface instabilities caused by shear between the liquid and air during motion. Conversely, the presence of a hole plate significantly enhances the breakup process and disintegrates liquid core into larger ligaments and

droplets. Additionally, the spray cone angle increases markedly from 8 degrees to 30 degrees, measured at a 90 mm axial distance from the nozzle tip, as anticipated.

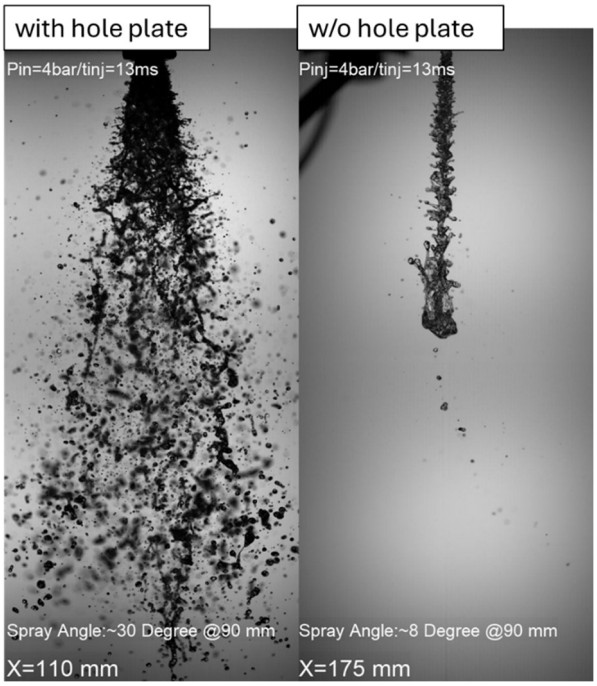

Figure 6. Far-field spray morphologies of Injector A *using hole plate and without hole plate* under 4 bar injection pressure at ca. 110 mm axial location from nozzle tip.

Although the spray atomization process was enhanced by incorporating a hole plate in the Injector A, the formation of large ligaments and droplets still poses a risk of wall wetting in the intake ports, which can increase emissions. Therefore, it is necessary to explore other PFI injectors that provide superior atomization performance, aiming for droplet sizes smaller than 100 micrometers. The rationale for selecting this droplet size is that such small droplets can seamlessly flow with the intake air and evaporate more rapidly, thereby ensuring a better mixture for combustion.

3.1.2 Spray Morphology of Pressure Atomizer at Far-field (Inj. B)

The spray evolution of the second PFI test injector (Injector B) was examined under various injection pressure conditions ranging from 5 to 20 bar. As illustrated in Figure 7, the spray morphology under 5-bar injection pressure condition exhibits similarities to that observed in Injector A without a hole, displaying only a liquid core with surface instabilities and no liquid breakup. Conversely, at an injection pressure of 10 bar, the breakup process occurs further downstream. The length of the liquid breakup shortens gradually, and the atomization process improves as the injection pressure increases. Figure 7 shows the spray evolution at 7.93 milliseconds after start of injection by covering until 220mm axial distance.

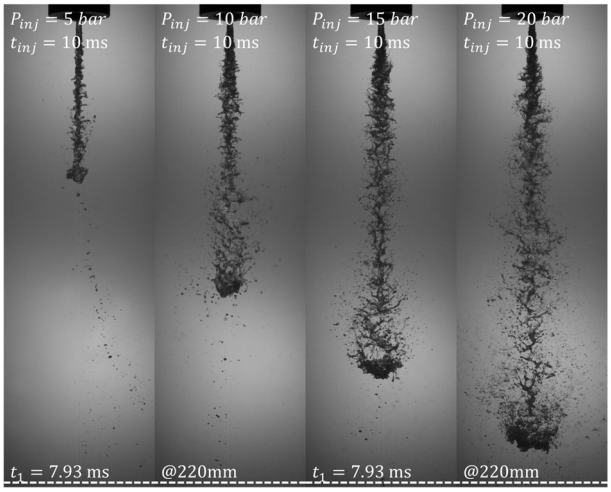

Figure 7. Far-field spray morphologies of pressure atomizer (Inj. B) under different injection pressure conditions (from 5 to 20 bar) at 220 mm axial location from nozzle tip.

Despite increasing the injection pressure up to the operational limit of the injector, the spray evolution predominantly exhibited large ligaments and bigger droplets with liquid coalescence at the spray tip front. Consequently, the atomization performance of this injector was inferior to that observed in the Injector A. Further investigation into the spray characteristics of the pressure-swirl atomizer will be detailed in the following section.

3.1.3 Near- and Far- Field Spray Morphologies of Pressure-Swirl Atomizer (Inj. C) and its Droplet Size Investigation Under Different Injection Pressure Conditions

Unlike the other two test injectors previously examined, injector C features a hollow cone design rather than a solid cone. This design employs internal swirl motion to enhance the spray breakup process. The investigation focused on the impact of varying injection pressures, ranging from 10 to 50 bar. It is evident that an increase in injection pressure results in greater spray tip penetration due to the higher momentum imparted to the spray. Additionally, at higher injection pressures, liquid sheets break up more rapidly, leading to improved atomization as illustrated in Figure 8. Following the breakup process, the spray predominantly disintegrates into significantly smaller droplets compared to the other two injectors. Figure 8 depicts the spray evolution 4.58 milliseconds after the start of injection, indicating axial distances of 60 and 180 mm to account for the intake port distance from the injector and prevent wall impingement.

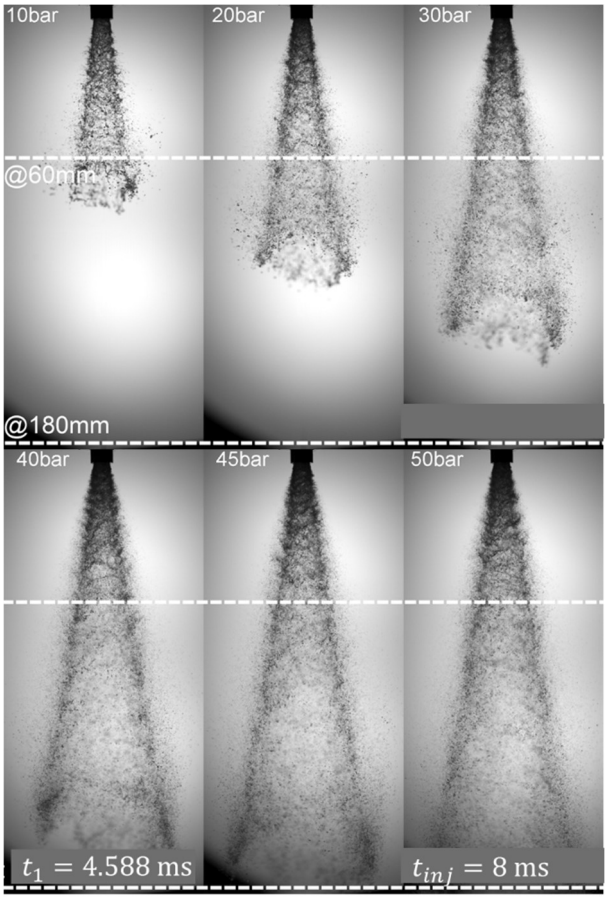

Figure 8. Far-field spray morphologies of pressure-swirl atomizer (Inj. C) for different injection pressure conditions (10 to 50 bar) at 180 mm axial distance from nozzle tip.

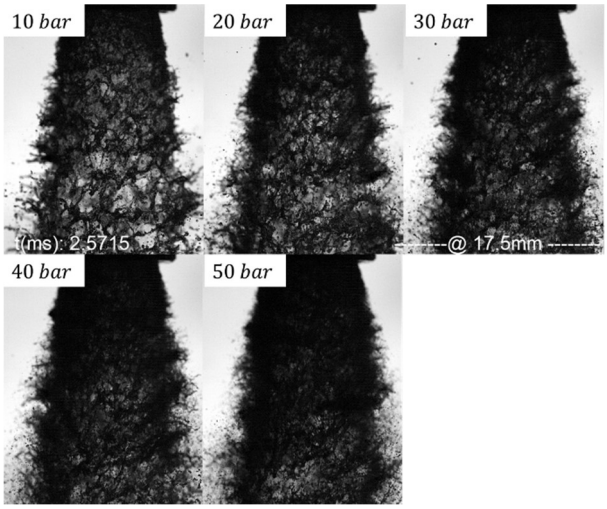

Figure 9. Near-field spray morphologies of pressure-swirl atomizer (Inj. C) for different injection pressure conditions (from 10 to 50 bar) at 17.5 mm axial distance nozzle tip.

In addition to observations in the far field, near-field spray morphologies were also investigated to understand the effects of swirl motion on the spray break-up process. Similar to the far-field observations, different injection pressures are used in this investigation, as shown in Figure 9. Near-field observations were conducted at 17.5 mm from the nozzle tip. Swirl characteristics generated inside the nozzle are clearly visible and significantly influence spray break-up in low-pressure conditions, as seen in the spray images taken at 2.57ms after the start of injection. This is attributed to the relatively low axial momentum of the spray. Conversely, the swirling structure at near-nozzle spray becomes less apparent at higher injection pressures because the increased injection pressure maintains the spray's axial direction, thereby not enhancing its radial momentum. Therefore, it can be considered that the impact of swirl motion on the breakup process is more significant under low-injection pressure conditions than under high-pressure conditions. Based on these far- and near-field observations, it is evident that the atomization performance of injector C surpasses that of injectors A and B.

The injector C produces significantly smaller droplets rather than disintegrating into ligaments compared to other test injectors. Droplet size confirmation was performed using microscopic imaging techniques. To avoid wall impingement in the intake port, we opted for lower injection pressure conditions to achieve short spray penetration. For this study, we utilized 10 and 20 bar injection pressures, evaluating droplet sizes at axial distances of 50 and 100mm. Figure 10 depicts the macroscopic spray images of injector C under 10 bar injection pressure conditions, along with corresponding droplet size images at 50mm and 100mm axial distances.

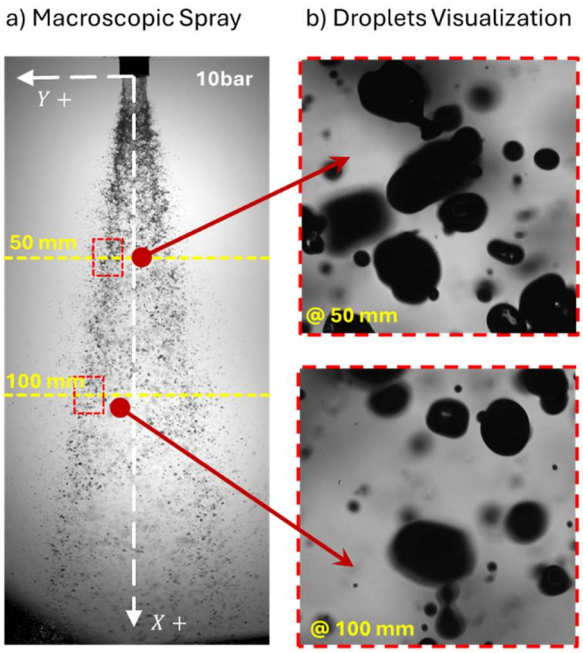

Figure 10. Droplet size imaging of pressure-swirl atomizer (Inj. C) under 10 bar injection pressure for different axial locations, a) microscopic spray morphology, b) droplets images at 50 mm and 100 mm axial distances from nozzle tip.

Droplet images are captured during the quasi-steady stage. For each injection, 10 images are captured, and for 5 consecutive injections, a total of 50 images are obtained. Droplet sizes are measured from these 50 images. The distribution and sizes of the droplets are presented as histogram plots in Figures 11 and 12. Detected number of smaller droplets are lower under the 10 bar injection conditions compared to the 20 bar injection conditions. This is attributed to the fact that high-velocity droplets can undergo secondary breakup more readily due to the aerodynamic forces generated between the air and liquid surface. From Figures 11 and 12, the average Sauter Mean Diameters (SMDs) are observed to be 517 micrometers at 50 mm and 480 micrometers at 100 mm under the 10 bar injection conditions. These droplet sizes are reduced to 411 and 360 micrometers for the 20 bar injections. It appears that such droplet sizes would still be relatively large. Therefore, such large droplets would not move seamlessly in the intake flow stream, as they may have difficulty evaporating quickly in the cold intake temperature. In that context, the effect of spray atomization performance of each test injector on engine performance and emissions will be investigated in the next section.

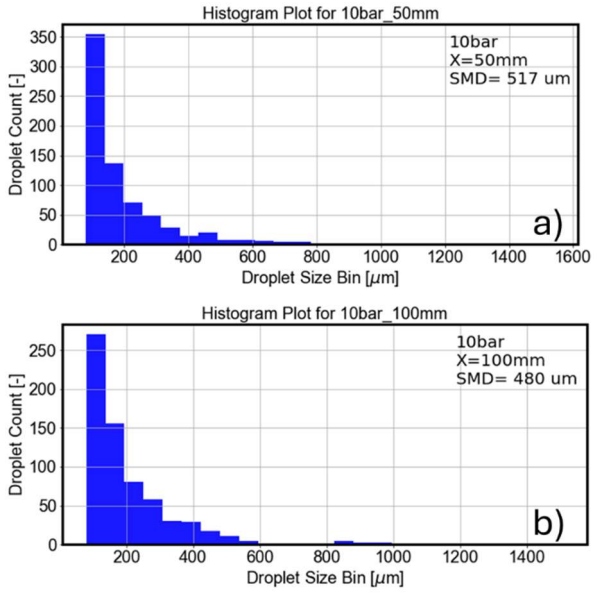

Figure 11. Droplet size distribution and average droplet size under **10 bar** injection pressure at *50 mm (a) and 100 mm (b) axial distance* from nozzle tip.

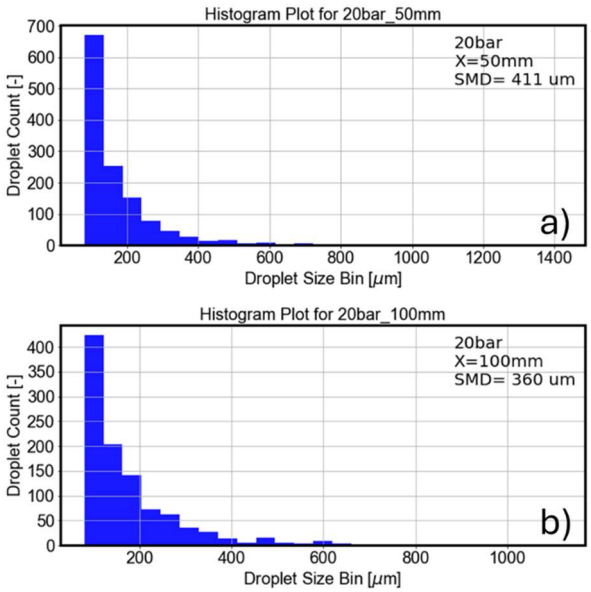

Figure 12. Droplet size distribution and average droplet size under **20 bar** injection pressure at *50 mm (a) and 100 mm (b) axial distance* from nozzle tip.

3.2 Effect of Different PFI Injectors (Spray Atomization Characteristics) on Engine Performance and Emissions

In this chapter, the impact of methanol fuel share and injector spray characteristic impact on engine performance is analyzed before the oxidation catalyst to understand what emissions the engine alone is producing, the oxidation catalyst performance is evaluated in the next chapter.

Fuel sharing is used, this means that diesel is the main fuel in terms of energy share and is injected directly into the combustion chamber and is burning with diffusion combustion like in a pure diesel engine while methanol is injected into each intake port and is pre-mixed with the intake air and evaporated during the compression stroke. The methanol is then ignited by the diesel close to TDC. The ultra lean and relatively cold (because of the evaporation) pre-mixed methanol/air mixture coming from fractional amounts of methanol under fuel-sharing strategy is challenging to burn completely when ignited by the main diesel fuel since the flame-front must propagate through this ultra lean mixture (see figure 13) even if the diesel is burning hot and rich locally around the diesel spray plumes.

It should be noted that for these investigations, only methanol share is varied, and all other settings are kept constant except for the methanol related injection parameters, wherein the best found setting for each injector is used.

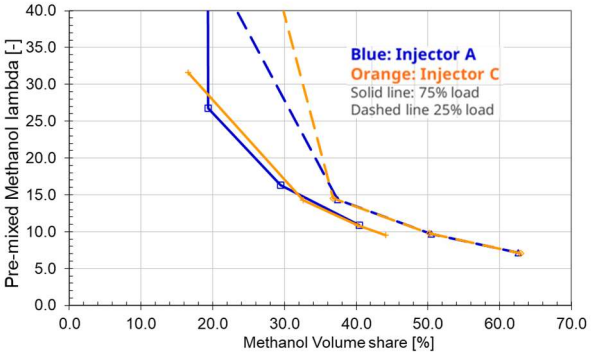

Figure 13. Pre-mixed methanol lambda versus methanol volume share, the pre-mixed methanol is extremely lean when the direct injected diesel is the main fuel.

Both methanol and formaldehyde emissions are strongly increased with an increased methanol share, see figure 14. This is also valid for carbon monoxide emission. However, the difference in emissions between injector A and injector C is very small even though the spray properties are completely different where injector C has superior spray quality.

The lower in-cylinder gas temperature because of the evaporation of the increasing pre-mixed methanol shares with high latent heat of evaporation, tend to form more unburned and partly burned emissions. This is mainly due to increased quenching close to cylinder walls where the premixed methanol flames are unable to burn since the main combustion itself is stronger with shorter combustion duration compared to pure diesel. Another reason for the increased emissions is that some of the homogenous air/fuel mixture is escaping during the scavenged period and some is trapped in crevices [20].

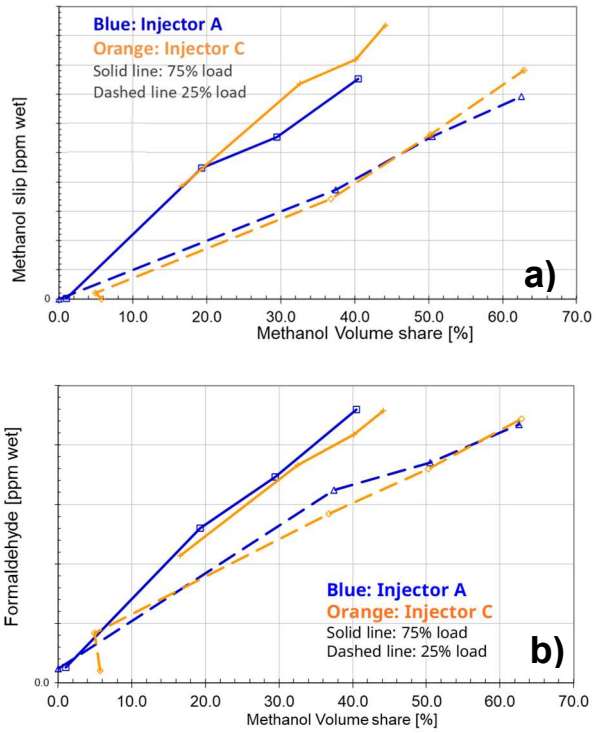

Figure 14. Methanol emission (a) and formaldehyde emissions (b) versus fuel share for injector A and C at different loads.

Overall NOx is typically reduced with increased methanol share, mainly because of the reduced temperature due to the high heat of evaporation of methanol. However, NO_2 emissions are increased with increased methanol share, see figure 15. The difference in NOx and NO_2 emissions between injector A and injector C is small even though spray properties are very different. The reason for the increased NO_2 is the more numerous presences of the HO_2 radical from methanol compared to diesel combustion [21]. During methanol oxidation significantly more HO_2 is formed compared to diesel, promoting the transformation of NO to NO_2.

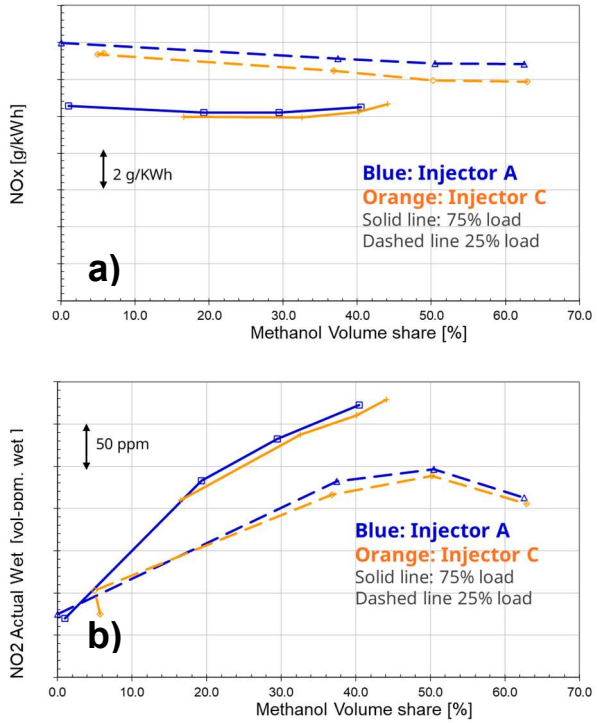

Figure 15. NOx emissions (a) and NO_2 emission (b) versus methanol share for injector A and C at different loads.

NO_2 is very toxic and has yellow/orange/red color depending on concentration. Orange smoke could be observed in the worst points with the highest NO_2 concentration during testing without any aftertreatment, see figure 16. SCR and/or oxidation catalyst is needed when running on methanol to reduce the NO_2 with this fuel-sharing combustion concept. However, when running on only DI diesel without SCR it is recommended to bypass the oxidation catalyst due to sensitivity for sulphur and the possibility that NO2 is produced.

Figure 16. Orange smoke could be observed in the worst points with the highest NO_2 concentration during testing without any aftertreatment

Even though there is almost no difference between the injector A and C in terms of emissions, a small difference in the peak heat release (when most of the pre-mixed MeOH is burned) between injector A and C is visible. Such difference is still surprisingly small when considering the big difference in droplet size and spray quality, see figure 17. The latter part of the combustion is mainly driven by the diesel injection rate and therefore the difference in late part of heat release is not as such affected by the PFI injector spray quality.

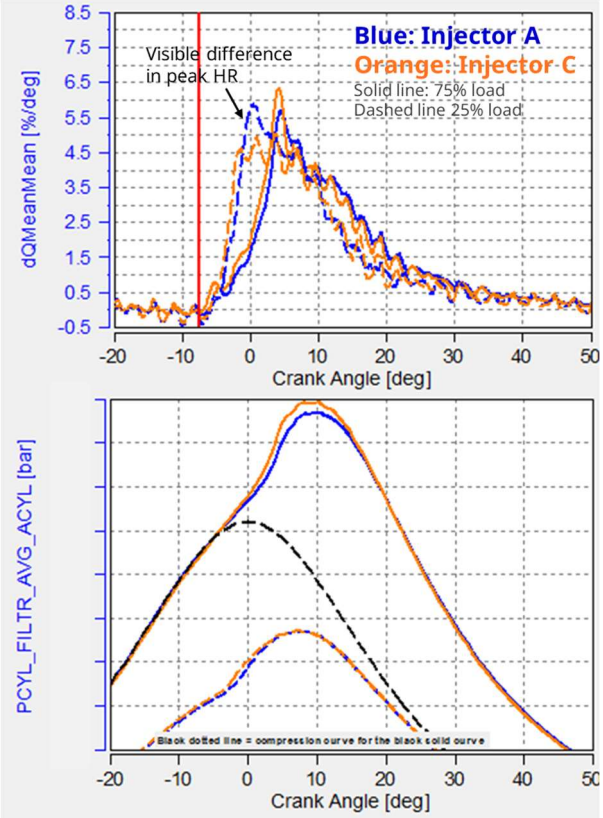

Figure 17. Heat release and firing pressure versus crank angle for injector A and C with about 40 vol% Methanol in all cases

The main limitation for increasing the methanol share is knocking and abnormal combustion especially if the target is to reduce the emissions without aftertreatment. Figure 18 shows the knocking tendency of methanol. Clearly, the knock amplitude is increasing exponentially with an increased methanol share. The most effective way to reduce the emissions is found to be the increased compression-end temperature, however, this also in turn causes an increase in knocking tendency. Nonetheless, if oxidation catalyst is employed and the compression-end temperature are reduced, the methanol share can be increased.

Were, the increased unburned fuel emissions from the combustion can be removed by the catalyst.

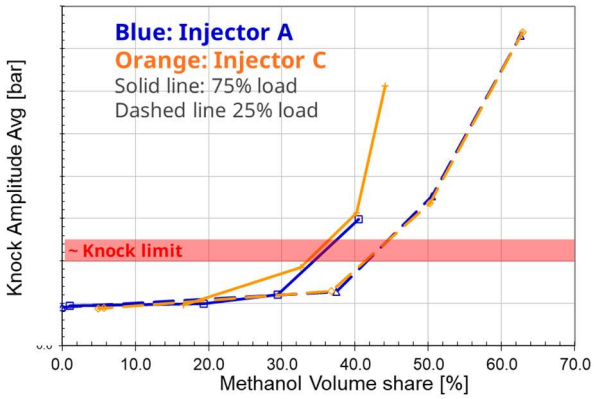

Figure 18. Knock amplitude versus methanol share for injector A and C at different loads.

As have been showed in above figures, the difference between injector A and C is small, and one possible explanation is that the very lean pre-mixed methanol remains difficult to burn even if the spray quality is improved. For examining this theory, it would be interesting to compare the two injectors in a fully pre-mixed otto combustion concept where methanol would be the main fuel and only a smaller amount of diesel would be used for pilot ignition of the methanol. In this case the pre-mixed methanol lambda would be much less extreme with better conditions for proper flame propagation. For doing this the compression ratio would need to be reduced significantly for avoiding knocking. Another possible reason for such small difference could be the fuel interactions with the hot intake valve, which is possibly naturalising the difference of initial droplet sizes to a large extent.

Based on the lube oil samples taken during the testing period, some methanol was detected in the lube oil. The methanol quantity was varying with varying operating conditions and consequently causing lube oil contamination. Indicatively, the lube-oil samples taken with injector C has in general a lower methanol content compared to injector A samples, probably due to the smaller droplet size with smaller inertia and less fuel ending up on cylinder walls.

Also, it should be noted that spray atomization performance in the current study although does not significantly impact emission reduction, an injector providing superior atomization performance could contribute to lower emissions. Especially in a fully pre-mixed otto combustion concept where methanol would be the main fuel and only a smaller amount of diesel would be used for pilot ignition of the methanol. In this case the pre-mixed methanol lambda would be much less extreme with better conditions for proper flame propagation. For doing this the compression ratio would need to be reduced significantly for avoiding knocking.

3.3 Oxidation Catalyst Performance

In terms of emissions, unburned methanol is not considered as a greenhouse gas, however, if an SCR is used, a fraction of the unburned methanol will oxidise into formaldehyde, which is highly toxic. About 5-20% of the unburned methanol is oxidised to formaldehyde in the SCR depending on load and temperature according to our previous experiments. In addition, some of the formaldehyde may chemically react with the SCR reagent Urea and form hydrogen cyanide (HCN). It is therefore important to limit the methanol slip entering the SCR, either by method of combustion or by using an oxidation catalyst.

SCR is needed for reaching IMO Tier III NOx level with this fuel sharing concept and the concern in this case is that the stack emissions of formaldehyde and hydrogen cyanide may be too high [22]. For this concept it is therefore proposed to introduce an oxidation catalyst before the SCR.

The oxidation catalyst is efficiently converting most of the methanol and carbon monoxide emissions at temperatures above 250 °C. Below 250 °C, there is a clear drop in conversion for both species.

Formaldehyde conversion is not as high as methanol and carbon monoxide conversion. Figure 19 shows a comparison between methanol, carbon monoxide and formaldehyde conversion levels at a mid-range engine load point. The exhaust gas temperature is varied by opening the exhaust waste-gate to reduce lambda and thereby increase the temperature.

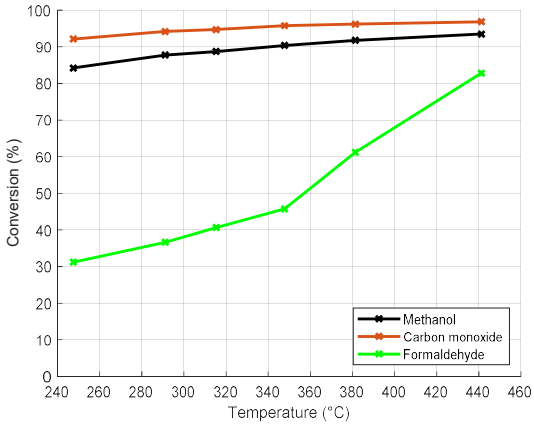

Figure 19. Comparison between methanol, carbon monoxide and formaldehyde conversion levels versus exhaust gas temperature at a mid-range engine load point.

Formaldehyde oxidation clearly has a higher light-off temperature than the other species. It can also be seen that the formaldehyde conversion is quite sensitive to exhaust flow or engine load. The reason for this is a mainly higher light-off temperature. Another reason is the methanol oxidation selectivity to formaldehyde, meaning that the oxidation of methanol may form some formaldehyde. This phenomenon is clearly visible at low temperatures and can be seen at ca 200 °C in figure 20, where a slight increase in formaldehyde is observed. This phenomenon suppresses the apparent formaldehyde oxidation mainly in the low temperature range.

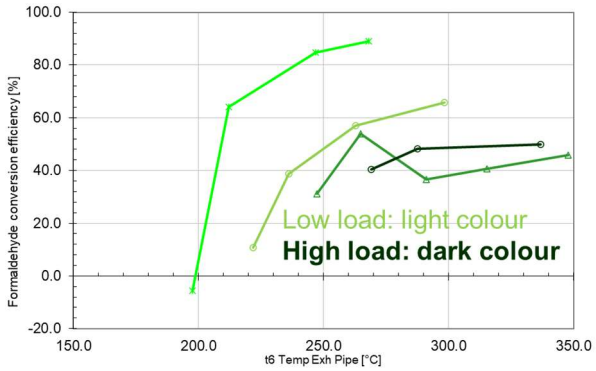

Figure 20. Formaldehyde conversion efficiency versus exhaust gas temperature.

The oxidation catalyst also influences NOx, more precisely the NO_2/NOx ratio. As is typical for Platinum Group Metal (PGM) catalysts, NO is oxidised to NO_2. When increasing the methanol concentration in the exhaust, the NO_2/NOx ratio at the catalyst inlet increases (see figure 15). On the other hand, the NO_2/NOx ratio decreases at the catalyst outlet, see figure 21. This is because NO_2 promotes the oxidation of methanol and its combustion products. As a result, NO_2 is converted back to NO. As the oxidation catalyst forms quite a bit of NO_2 when operating on only diesel it is not recommended to use this without an SCR due to the risk of visible and toxic NO_2 emissions. Furthermore, the PGM catalyst can be sensitive to sulphur, so the diesel fuel quality may need to be restricted if an oxidation catalyst is to be used.

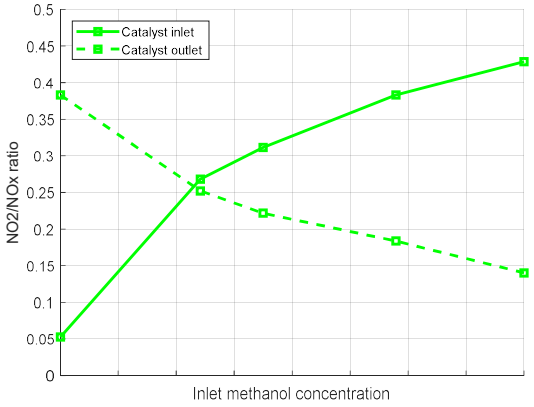

Figure 21. NO_2/NOx ratio versus methanol concentration at catalyst inlet (solid) and outlet (dashed).

3.4 Performance Comparison with and without Oxidation Catalyst

The target of the test activity is to investigate engine performance using the best injector (injector C) and compare a case when emissions are minimized from combustion itself without oxidation catalyst (orange case) to a case when methanol share is maximized, and a small oxidation catalyst is introduced to allow increased methanol share (green case) and still have low emissions after the catalyst. The comparison is done at similar knock and formaldehyde level since these are the main limitations in both cases.

Emissions from combustion itself is increased with increased methanol share and so are also the knocking tendency. To allow the increased methanol share, engine settings are relaxed by reducing the compression end temperature and by phasing combustion somewhat later, this is increasing the emission further. By doing this the methanol share could be increased about 30% units at low and part load, see figure 22. At full load there is no margin to increase the methanol share because of firing pressure limitations.

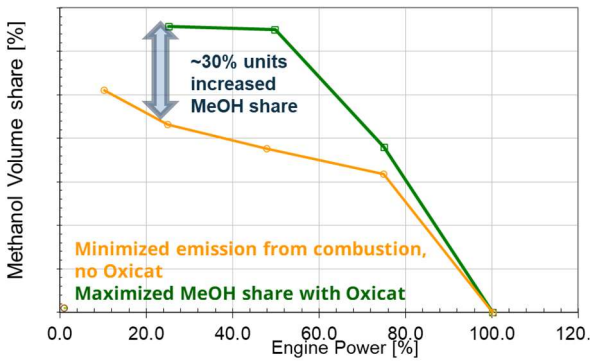

Figure 22. Methanol volume share versus engine load, methanol share can be increased up 30% by using oxidation catalyst.

Significant emission reduction can be achieved by using oxidation catalyst despite the increased emission from combustion itself. Among the evaluated emissions, CO is the easiest emission to oxidise and therefore the largest improvement can be observed in this emission. The level after the oxidation catalyst becomes very low, see figure 23(a). Methanol slip is also oxidised very well as seen in chapter 3.3 down to acceptable level, see figure 23(b). NO_2 is reduced by the oxidation catalyst down to a level that removes the need of SCR to reduce NO_2 when running at IMO Tier II NOx level (SCR is still needed for possible Tier III operation), see figure 23(c). The tested oxidation catalyst volume is sufficient for all emissions except formaldehyde. To reduce formaldehyde to a good level, the volume would need to be increased.

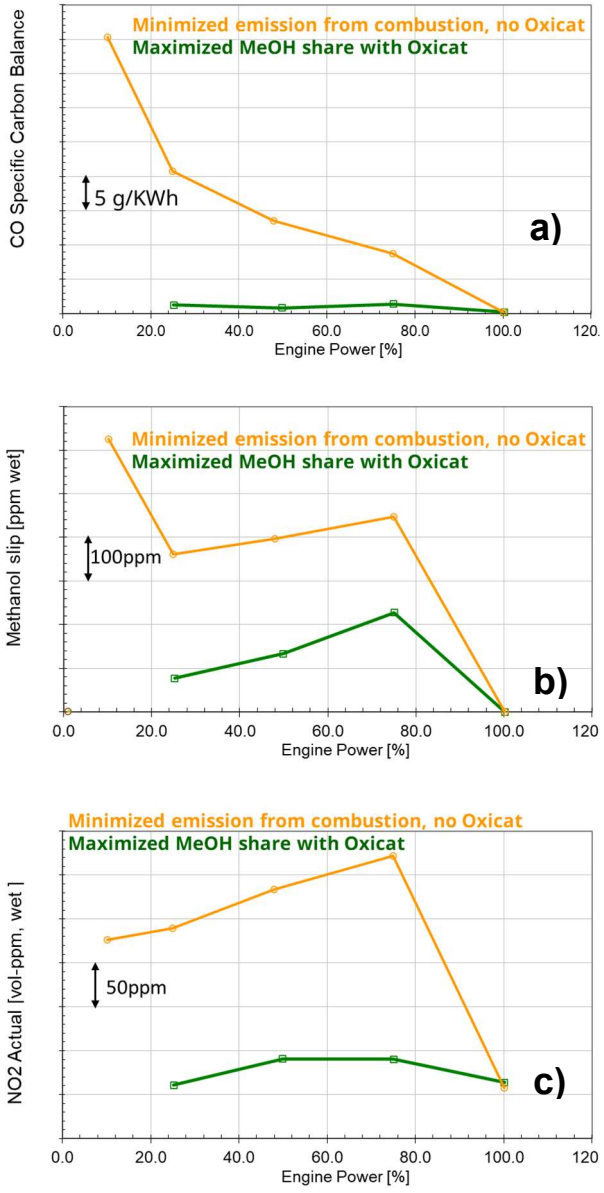

Figure 23. Carbon monoxide emission (a), Methanol emission (b) and Nitrogen dioxide emission (c) versus engine load.

4 CONCLUSIONS

This study examined port fuel injected methanol and its potential aftertreatment concepts to reduce both regulated and unregulated emissions with respect to methanol fuel share concept. The research focused on optimizing methanol spray and determining the maximum methanol share. Initially, the atomization performance of three different PFI injectors was assessed. Subsequently, the effects of the atomization characteristics of PFI injectors and methanol share were correlated with engine emissions using a medium-speed four-stroke research engine. The unburned and partly burned emissions are strongly increased with increased fuel share therefore an oxidation catalyst was accordingly examined. Its impact on emission characteristics and conversion efficiency is evaluated on the test engine with respect to exhaust gas temperature to assess the needed temperature for reaching good conversion efficiency. Finally, the combination of engine and oxidation catalyst performance with the best injector is evaluated and possible issues when combined with SCR discussed. The key findings based on the results are summarized below:

- Injector A and B generates mostly ligaments and large droplets whereas injector C produces relatively smaller droplets without any large ligaments due to promotion of swirl-effect on the spray dynamics under the low injection pressure conditions.
- Relatively smaller droplets emerged from injector C has a negligible effect on the emission compared to injector A. This finding was discussed considering two possible explanations: first, very lean pre-mixed methanol would remain difficult to burn, even with enhanced atomization. Second, the significant interaction between the spray and hot intake valves could neutralize the effect of droplet size on emissions.
- On the other hand, smaller droplets produced by injector C results in less methanol in the lube oil compared to injector A which is important for avoiding lube oil contamination.
- All unburned and partly burned emissions are increased with increased methanol share mainly due to the reduced compression end temperature due to the evaporation of methanol and thereby giving increased quenching.

- Regarding the aftertreatment concepts, it is recommended to introduce an oxidation catalyst (Oxicat) before the selective catalytic reduction (SCR) to mitigate formaldehyde (toxic unregulated emission) formation and its reaction with Urea in SCR which can result in hydrogen cyanide (HCN).

- NO2 emission is also increased with increased methanol share while overall NOx is reduced. To prevent excessive toxic NO2 and even orange smoke, an oxidation catalyst or SCR is needed.

In summary, this paper demonstrates that spray characteristics and aftertreatment is crucial for achieving low methanol emissions. It confirms that both regulated and unregulated emissions can be minimized with a suitable sized oxidation catalyst before the SCR Furthermore, it facilitates the straightforward conversion of existing diesel engines to methanol operation.

As a future work, the effort will be exerted to investigate pre-mixed methanol otto combustion strategies to build up clear understandings how spray atomization impacts emissions and engine performance.

5 ABBREVIATIONS

CFD – Computational Fluid Dynamics

CPSI – Cells Per Square Inch

DBI – Diffuse Backlight Illumination

DI - Direct injection

GHG - Greenhouse gas

HO_2 - Hydroperoxyl radical

HCN - Hydrogen cyanide

ICE - Internal combustion engine

IMO – International Maritime Organization

LFO –Light Fuel Oil

NOx – Nitrogen Oxides

NO2 – Nitrogen dioxide

Oxicat – Oxidation catalyst

PFI - Port fuel injection

PGM – Platinum Group Metal

PM - Particulate Matter

SCR - Selective Catalytic Reduction

SMD - Sauter Mean Diameter

SOI – Start of Injection

TDC – Top Dead Center

6 ACKNOWLEDGMENTS

A special thanks goes to SC 6L20 research engine test team, fuel injection team and the fuel rig team for all their effort during the test campaigns that this paper is based on.

7 REFERENCES AND BIBLIOGRAPHY

[1] Tripathi, S., Gorbatenko, I., Garcia, A., & Sarathy, M. (2023). Sustainability of Future Shipping Fuels: Well-to-Wake Environmental and Techno-Economic Analysis of Ammonia and Methanol (No. 2023-24-0093). SAE Technical Paper.

[2] Rezaei, R., Hayduk, C., Fandakov, A., Rieß, M., Sens, M., & Delebinski, T. O. (2021). Numerical and experimental investigations of hydrogen combustion for heavy-duty applications (No. 2021-01-0522). SAE Technical Paper.

[3] Matsunaga, D., Tentora, T., Hiraoka, K., & Toshinaga, K. (2023). A Study on Combustion and Emission Characteristics of Ammonia, Hydrogen and Diesel Tri-Fuel Engines (No. 2023-32-0103). SAE Technical Paper.

[4] Repo, J., Axelsson, M., & Heir, V. (2023, June). Methanol combustion concept alternatives for new build and retrofit of 4-stroke medium speed engines. In Proceedings of the 30th CIMAC World Congress, Busan, Republic of Korea (pp. 12-16).

[5] Tian, Z., Wang, Y., Zhen, X., & Liu, Z. (2022). The effect of methanol production and application in internal combustion engines on emissions in the context of carbon neutrality: A review. Fuel, 320, 123902.

[6] Zhen, X., & Wang, Y. (2015). An overview of methanol as an internal combustion engine fuel. Renewable and Sustainable Energy Reviews, 52, 477-493.

[7] Li, X., Yan, P., Li, H. M., Zheng, L., Shen, G., Hu, Y. C., & Han, D. (2023). Numerical Study of the Effect of Direct-Injection Timing of Methanol and Excess Air Ratio on the Combustion Characteristics of a Marine Diesel-Methanol Dual-Fuel Engine (No. 2023-01-1626). SAE Technical Paper.

[8] Zhao, Y., Liu, X., & Kook, S. (2024). Combustion Mode Evaluation of a Methanol–Diesel Dual Direct Injection Engine with a Control of Injection Timing and Energy Substitution Ratio. SAE International Journal of Engines, 18(03-18-01-0002).

[9] Chen, H., Su, X., He, J., & Xie, B. (2019). Investigation on combustion and emission

characteristics of a common rail diesel engine fueled with diesel/n-pentanol/methanol blends. Energy, 167, 297-311.

[10] Yao, C., Cheung, C. S., Cheng, C., Wang, Y., Chan, T. L., & Lee, S. C. (2008). Effect of diesel/methanol compound combustion on diesel engine combustion and emissions. Energy conversion and management, 49(6), 1696-1704.

[11] Singh, I., Güdden, A., Raut, A., Dhongde, A., Emran, A., Sharma, V., & Wagh, S. (2024). Experimental and Numerical Investigation of a Single-Cylinder Methanol Port-Fuel Injected Spark Ignition Engine for Heavy-Duty Applications (No. 2024-26-0072). SAE Technical Paper.

[12] Lu, X., Wu, T., Ji, L., Ma, J., & Huang, Z. (2009). Effect of port fuel injection of methanol on the combustion characteristics and emissions of gas-to-liquid-fueled engines. Energy & fuels, 23(2), 719-724.

[13] Wang, Y., Xiao, G., Li, B., Tian, H., Leng, X., Dong, D., & Long, W. (2022). Study on the performance of diesel-methanol diffusion combustion with dual-direct injection system on a high-speed light-duty engine. Fuel, 317, 123414.

[14] Catapano, F., Di Iorio, S., Magno, A., Sementa, P., & Vaglieco, B. M. (2023). A Comparison of Methanol, Methane and Hydrogen Fuels for SI Engines: Performance and Pollutant Emissions (No. 2023-24-0037). SAE Technical Paper.

[15] Wu, Y., Wang, C., Huang, Z., Wang, W., Jin, C., Zhang, Z., ... & Yao, M. (2024). The combustion and emission characteristics of pure methanol as a substitute fuel for compression ignition engines. International Journal of Green Energy, 21(14), 3313-3329.

[16] Cheung, C. S., Zhang, Z. H., Chan, T. L., & Yao, C. (2009). Investigation on the effect of port-injected methanol on the performance and emissions of a diesel engine at different engine speeds. Energy & fuels, 23(11), 5684-5694.

[17] Güdden, A., Pischinger, S., Geiger, J., Heuser, B., & Müther, M. (2021). An experimental study on methanol as a fuel in large bore high speed engine applications–Port fuel injected spark ignited combustion. Fuel, 303, 121292.

[18] Koebel, M., Elsener, M., & Kleemann, M. (2000). Urea-SCR: a promising technique to reduce NOx emissions from automotive diesel engines. Catalysis today, 59(3-4), 335-345.

[19] Castrejón-García, R., Castrejón-Pita, J. R., Martin, G. D., & Hutchings, I. M. (2011). The shadowgraph imaging technique and its modern application to fluid jets and drops. Revista mexicana de física, 57(3), 266-275.

[20] Dierickx, J., Verbiest, J., Janvier, T., Peeters, J., Sileghem, L., & Verhelst, S. (2021). Retrofitting a high-speed marine engine to dual-fuel methanol-diesel operation: A comparison of multiple and single point methanol port injection. Fuel Communications, 7, 100010.

[21] Lu, H., Yao, A., Yao, C., Chen, C., & Wang, B. (2019). An investigation on the characteristics of and influence factors for NO2 formation in diesel/methanol dual fuel engine. Fuel, 235, 617-626.

[22] Elsener, M., Nuguid, R. J. G., Kröcher, O., & Ferri, D. (2021). HCN production from formaldehyde during the selective catalytic reduction of NOx with NH3 over V2O5/WO3-TiO2. Applied Catalysis B: Environmental, 281, 119462.